Chemical Engineering Science 202 (2019) 26–35

Contents lists available at ScienceDirect

Chemical Engineering Science

journal homepage: www.elsevier.com/locate/ces

The nanoscale dimension determines the carbonization outcome of electrospun lignin/recycled-PET fibers

Efstratios Svinterikos [a], Ioannis Zuburtikudis [b,*], Mohamed Al-Marzouqi [a]

[a] Department of Chemical and Petroleum Engineering, United Arab Emirates University (UAEU), P.O. Box 15551, Al Ain, United Arab Emirates
[b] Department of Chemical Engineering, Abu Dhabi University (ADU), P.O. Box 59911, Abu Dhabi, United Arab Emirates

HIGHLIGHTS

- The carbonization of lignin/PET fibrous mats yields different carbon morphologies based on their average fiber diameter.
- Thick submicron fibers (>387 nm) are infusible during carbonization and yield a fibrous carbon structure.
- Nanofibers of minimum diameter (80 nm) melt and yield a fused carbon structure.
- The nano-diameter maximizes the heat and mass transfer in the process and the decomposition rate of lignin macromolecules.
- DSC shows variations in the enthalpy of fusion triggered by the nano-diameter.

GRAPHICAL ABSTRACT

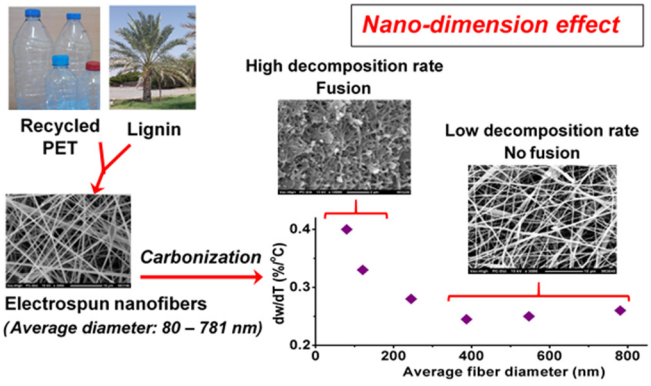

ARTICLE INFO

Article history:
Received 26 November 2018
Received in revised form 1 March 2019
Accepted 7 March 2019
Available online 11 March 2019

Keywords:
Carbon nanofibers
Diameter
Carbonization
Electrospinning
Lignin
Recycled PET

ABSTRACT

The impact of the nanoscale dimension on the carbonization of electrospun fibers is usually overlooked. In this study, we prove that it is a decisive factor in the outcome of the carbonization process. Six electrospun fibrous mats, each with a different average fiber diameter ranging from 80 nm to 781 nm were fabricated from a lignin/recycled-PET blend of mass ratio 1/1, and their weight loss and decomposition profile were monitored via thermogravimetry. The nano-size effect is evident for those electrospun mats with average diameter lower than 121 nm. These mats exhibit a significantly higher decomposition rate at the 180–260 °C temperature range, which leads to a considerable degree of fusion of the precursor nanofibers. Thus, the carbon structures formed from these mats do not retain the geometrical integrity of their precursor nanofibers. In contrast, no size-effects are manifested to the electrospun samples of average fiber diameter larger than 387 nm, as they decompose at a similar and lower rate between 180 and 260 °C and yield infusible carbon fibers with similar geometry as their corresponding precursor fibers. These results highlight the determinant role of the nano-dimension when carbon fibers are produced through the carbonization of precursor fibers at the sub-micron scale and point out its significance in processes controlled by heat and mass transfer phenomena, as in the case of carbonization.

* Corresponding author.
E-mail address: ioannis.zuburtikudis@adu.ac.ae (I. Zuburtikudis).

https://doi.org/10.1016/j.ces.2019.03.013
0009-2509/

1. Introduction

Carbon fibers are a high value-added form of carbon, which is suitable for a variety of large-scale applications, such as for manufacturing composites for the automotive and the aerospace sectors, for energy storage, adsorption, catalysis and tissue engineering among others (Zhang et al., 2016; Peng et al., 2016; Frank et al., 2014; Inagaki et al., 2012). Typically, their structure consists of graphitic and amorphous regions, and they carry an array of attractive properties such as high specific surface area, superior tensile strength and modulus that can reach up to four times that of steel, combined with much lower specific gravity, high thermal stability and electrical conductivity. In addition, they have demonstrated a remarkable flexibility in designing their properties based on the desired application (Zhang et al., 2016; Frank et al., 2014; Ogale et al, 2016). They are primarily manufactured through the spinning and the thermal treatment of polymeric precursors, mainly poly (acrylonitrile), or alternatively via chemical vapor deposition (Zhang et al., 2016; Peng et al., 2016). Their structure and properties are based on various controllable factors such as the choice of the precursor materials, the spinning procedure, the conditions of thermal treatment and the presence of additives among others.

More precisely, when their diameter is decreased in the nanoscale, they are termed as carbon nanofibers (CNFs), which are suitable for applications such as adsorption or catalysis, where the nano-size dimension and the specific surface area play a major role. Therefore, when attempting to manufacture carbon nanofibers, it is important to carefully select the process conditions in order to achieve the desirable nanofibrous structure.

A suitable technique for producing precursor polymer nanofibers is electrospinning. Its main advantages lie in its simplicity and its versatility in producing desirable nano-sized fibers by easily adjusting the process conditions (Peng et al., 2016; Svinterikos and Zuburtikudis, 2017). The precursor polymer nanofibers are subsequently transformed into CNFs by heating them at elevated temperatures (typically >600 °C) under inert atmosphere. Sometimes, a stabilization step of heating at moderate temperature (around 200 °C) precedes the carbonization step in order to render the precursor fibers infusible (Frank et al., 2014; Inagaki et al., 2012).

The most common polymeric precursor of CNFs via electrospinning is poly(acrylonitrile) (Frank et al., 2014; Inagaki et al., 2012). Due to its relatively high cost however, alternative inexpensive and renewable raw materials have been used for CNF preparation. One of them is lignin, the second most abundant natural polymer on earth behind cellulose (Frank et al., 2014; Ruiz-Rosas et al., 2010). The suitability of lignin as a CNF precursor is justified by its relatively high-carbon content, its availability and the absence of toxic by-products during its thermal treatment (Frank et al., 2014). Depending on its plant source and its extraction process, the configuration of its structure and its properties vary, but typically it consists of a network of phenylpropane units (Frank et al., 2014; Ogale et al., 2016). Due to its relatively low molecular weight, lignin sometimes exhibits spinnability difficulties during electrospinning. In this case, a binder polymer is necessary for the formation of electrospun nanofibers. Previous research reports of our team (Svinterikos and Zuburtikudis, 2016) have demonstrated that recycled poly(ethylene terephthalate) (PET) is appropriate for this purpose, and CNFs can be produced after carbonizing the precursor electrospun nanofibers. Carbon microfibers based on a blend of lignin with PET have also been reported in the literature (Kubo and Kadla, 2005; Compere et al., 2005), but in that case the precursor fibers were fabricated via melt spinning. PET is a widely-used commodity polymer and the most widely recycled plastic in the USA in terms of weight (NAPCOR, 2018). Therefore, alternative uses of recycled PET can have a positive environmental impact.

Lignin is a highly branched polymer; therefore, its thermal decomposition (devolatilization) under inert atmosphere is slow and is extended over a long temperature range in a multi-stage process. Typically, it exhibits an intense decomposition regime close to 300 °C, a second regime around 560 °C and a third regime over 700 °C (Chin et al., 2014; Rodríguez Correa et al., 2017). During this process, oxygen and hydrogen atoms are released, mainly in the form of CO, CO_2, H_2, CH_4, and phenolic compounds (Rodríguez Correa et al., 2017; Kim et al., 2016; Mohabeer et al., 2017). The final solid residue mainly consists of polyaromatic graphitic and disordered carbon (Rodríguez Correa et al., 2017). PET on the other hand decomposes at a very narrow temperature range, with the maximum rate of decomposition appearing around 400–480 °C depending on the heating rate and the polymer grade (Brems et al., 2011; Ko et al., 2014; Przepiórski et al., 2009).

In this research, we prepared precursor electrospun fibrous samples of varying average fiber diameter and we monitored their carbonization, by recording their weight loss via thermogravimetry (TGA). The effect of lowering the average diameter to the nanoscale, although it may significantly influence the transformation into CNFs, has scarcely been reported in the literature. Ye et al. (2015) have reported that PAN-based electrospun nanofibers of 39 nm average diameter exhibited a higher weight loss during carbonization, compared to thicker nanofibers, although this was not the main focus of their study. Here we present and discuss our findings, for the case of lowering the average diameter of electrospun lignin/recycled-PET fibers up to 80 nm and for the subsequent production of carbon fibers.

2. Materials and methods

Kraft lignin was purchased from Sigma-Aldrich (#471003, CAS No 8068051, Mw ~ 10,000 g/mol, low sulfonate content) and was used as received. The source of recycled PET (r-PET from now on) was waste water bottles, which came from the same bottling company in the U.A.E. Prior to the preparation of the spinnable solutions the bottles were left to dry and then they were cut into small pieces. The Melt Flow Index (MFI) of r-PET was measured to be 72 g/10 min at 265 °C with 2.16 kg load (measurement with a Chengde Jingmi (XRL-400) plastometer according to ASTM D1238). The solvent used in the electrospinning process was trifluoroacetic acid (TFA, 99%) purchased from Merck. The solutions of lignin/r-PET were prepared and left under magnetic stirring at room temperature for 12 h until homogeneously dissolved.

The electrospinning process was performed in a FUENCE E-sprayer (ES-2000S) apparatus in which the setup has vertical orientation. For the preparation of electrospun mats with a predetermined range of the average fiber diameter, a design-of-experiments statistical methodology was applied. Details on the methodology that we followed in order to optimize the process can be found elsewhere (Svinterikos and Zuburtikudis, 2017). For the purpose of examining the role of the fiber diameter in their carbonization rate, six electrospun mats of different average fiber diameter were prepared. All of them consisted of lignin/r-PET with a mass ratio of 1/1. The six mats consisted of submicron- and nano-sized fibers, with the following average fiber diameter and standard deviation for each mat: (1) 80 ± 21 nm, (2) 121 ± 38 nm, (3) 245 ± 79 nm, (4) 387 ± 148 nm, (5) 547 ± 205 nm, (6) 781 ± 284 nm. For simplification, in the following paragraphs only the average fiber diameter will be mentioned for each mat. Histograms showing the diameter distribution for each of the electrospun and carbonized mats are displayed in the Supplementary Material (SM) (Table S2). The electrospinning conditions that led

to the preparation of each sample are presented in the SM, as well (Table S1 in the SM).

Pristine commercial lignin could not be electrospun into fibers due to its relatively low molecular weight (Svinterikos and Zuburtikudis, 2016). When pure lignin was used, there was only electrospray instead of fibers. The carbonization of this electrosprayed lignin was also monitored for comparison purposes. In addition, a sample consisting of electrospun fibers of pure r-PET with average fiber diameter of 204 ± 90 nm was prepared, and its thermogravimetric profile was recorded.

The electrospun mats were carbonized in a temperature-programmed tubular furnace (Tube Furnace GSL-1500X-50, MTI). Each sample was heated under inert atmosphere (N_2) at a heating rate of 5 °C/min until it reached 600 °C, where it was held for 1 h.

The morphology of the electrospun and of the carbonized samples was examined with Scanning Electron Microscopy (SEM) (JEOL Neoscope JCM-5000) after they were gold-coated. Their diameter distribution was measured using an image analyzer (ImageJ, National Institute of Health, U.S.A.). Around 200 fiber diameters were measured at different spots of each sample in order to ensure representative measurements.

The carbonization rate of the electrospun fibers was investigated via Thermogravimetric Analysis (TGA) using a TA Q500 instrument. Around 6–10 mg of each sample were heated under inert atmosphere with a rate of 7 °C/min from 25 till 900 °C. N_2 was used as a carrier gas with a flow rate of 40 mL/min. Differential Scanning Calorimetry (DSC) tests were carried out at inert atmosphere (N_2) with a heating rate of 7 °C/min, using a TA DSC25 instrument. Elemental analysis with Energy Dispersive X-Ray Spectroscopy (EDS) was performed using a JEOL JSM-6010PLUS scanning electron microscope.

3. Results and discussion

3.1. The decomposition profiles of lignin and of r-PET

Fig. 1 shows the decomposition of pristine lignin in comparison with that of the electrosprayed lignin. Pristine lignin undergoes a multiple-stage decomposition, the first stage of which is located between 154 and 400 °C (after the removal of moisture at T < 100 °C). At this wide stage, the cleavage of weaker bonds (e.g. C–O) takes place with the maximum rate of decomposition appearing at 295 °C. The asymmetrical shape of this peak indicates the diversity of the decomposition reactions taking place, which is due to the irregular structure of lignin. The evolution of medium-volatile constituents continues until around 600 °C, above which the final stage of lignin decomposition takes place, with the cleavage of stronger bonds (e.g. C – H) (Kim et al., 2016; Chen et al., 2016). This profile is in accordance with similar curves for commercial lignin found in the literature (Chin et al., 2014; Rodríguez Correa et al., 2017).

Inspection of Fig. 1 shows clearly that the first stage of decomposition of electrosprayed lignin is much different than that of the pristine one. Between 185 and 267 °C there is a significant weight loss, followed by a smaller weight loss between 267 and 400 °C. In the first of these two regimes, the rate of weight loss reaches the peak value of 0.56%/°C at 237 °C, which is much higher (more than double) than that at the peak of pristine lignin (0.25%/°C at 295 °C). These differences in the two profiles, indicate that electrosprayed lignin decomposes faster compared to the pristine one, and a larger amount of volatile gases evolve from its bulk. The second regime reaches its highest value of decomposition rate (0.17%/°C) at 307 °C. At 400 °C, the residual weight is 51.5% and 65% for the electrosprayed and the pristine lignin respectively. Above this temperature, there is no significant change in DTG curve between these two materials, but electrosprayed lignin keeps decomposing at a slight higher rate. The final yield at 900 °C is 8.6% and 29% respectively.

It has been reported that trifluoroacetic acid, the electrospinning solvent used in this study, induces changes in the lignin molecular structure (Svinterikos and Zuburtikudis, 2016; García et al., 2009), which are associated with oxidation of aryl-carbon atoms or attachment of fluoride ions on them, and possibly with some rearrangement of their peripheral groups. Obviously, these changes have an impact on the carbonization profile of lignin.

In addition, the most important reason for the difference in the decomposition profiles between the two samples, is most probably the large size difference between their granules. Fig. 2(a) shows

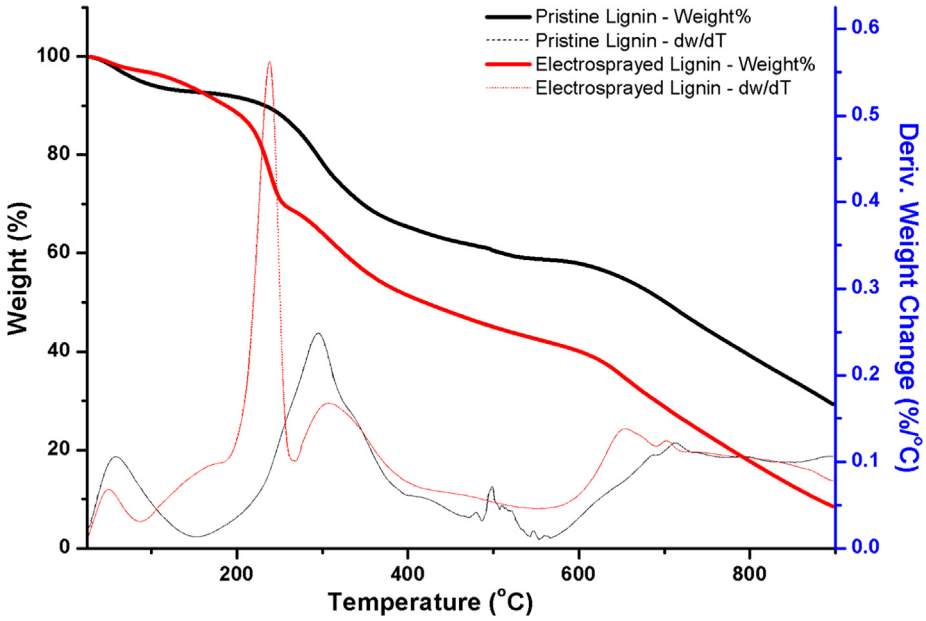

Fig. 1. Weight loss as a function of temperature for the pristine lignin (black) and for the electrosprayed lignin (red). The dotted lines display the first derivative of the weight loss. (For interpretation of the references to colour in this figure legend, the reader is referred to the web version of this article.)

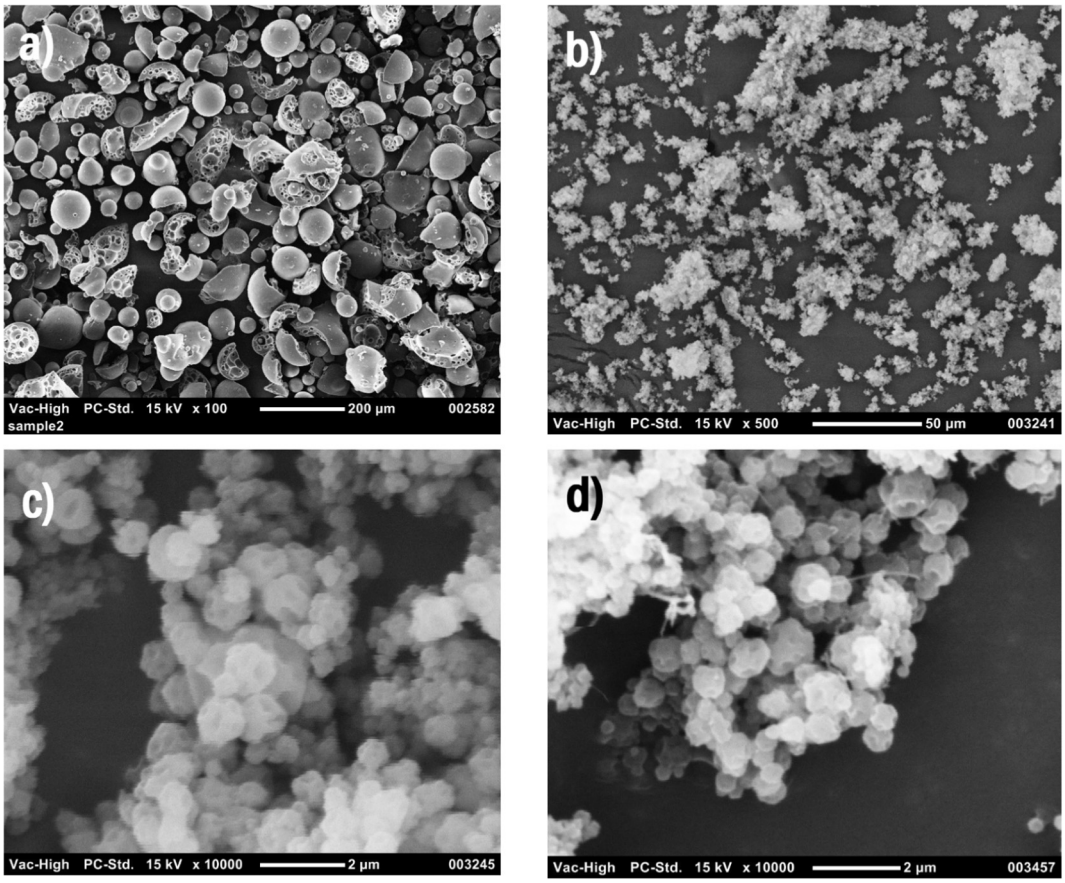

Fig. 2. Granules of (a) pristine lignin (magnification ×100), (b) electrosprayed lignin (×500), (c) electrosprayed lignin (×10,000), (d) carbonized electrosprayed lignin (×10,000).

that pristine commercial lignin consists of large granules with an average size that was measured to be 56.4 ± 24 µm. In contrast, the electrospinning process produces spray of very small droplets, which after deposition on the collector and evaporation of the solvent, results in the formation of submicron-sized rough granules of electrosprayed lignin (Fig. 2(b) and (c)). The average diameter of these granules was measured to be 669 ± 228 nm. This almost hundred-fold decrease in the average size of lignin particles results in a vast increase in the total surface area per unit mass. More precisely, and assuming spherical granules and by simple geometrical calculations, decreasing their average diameter by 84.3 times, increases their specific surface area by around 7106 times. Since the decomposition process is dependent on heat transfer towards the interior of the particles and mass transfer from their interior to the atmosphere, such a massive increase in the surface area of the granules is expected to speed up the whole process. The reason is that more molecules are on the surface or near the surface of the granules, and the volatile gases can escape faster through diffusion from their core. Indeed, the TGA profiles of these two samples demonstrate this effect.

Moreover, the complex irregular structure of lignin results in the absence of melting temperature (Svinterikos and Zuburtikudis, 2016). In the case of the carbonization of lignin/r-PET fibers, this property of lignin is desirable, since it allows the preservation of the fibrous structure, as the fibers are slowly carbonized without melting. Fig. 2(d) shows the electrosprayed lignin after having been carbonized at 800 °C under inert atmosphere. The granules retain their shape, while their size distribution remains at the same levels as of the starting electrosprayed ones (622 ± 213 nm).

Using lignin alone, it was not feasible to produce electrospun fibers. This is attributed to the relatively low molecular weight of the lignin used here, which results in the absence of extensive chain structures and molecular entanglements (Dallmeyer et al., 2010). This in turn results in lignin solutions of relatively low viscosities, or at least lower than the values required for the successful formation of fibers. For the electrospinning technique, it is well known that if the viscosity of the solution is relatively low then the jet breaks into droplets under the influence of the electrostatic field (Ko and Wan, 2014). Therefore, it was not possible to produce lignin nanofibrous mats of different average fiber diameters and to compare their decomposition rates.

Fig. 3 presents the TGA curve of the starting r-PET as well as that of the electrospun r-PET. The fibrous mat of electrospun r-PET consisted of fine fibers with average fiber diameter of 204 ± 90 nm (see Fig. S1 in the SM). Here the behavior is totally different than in the case of lignin. Both samples exhibit an almost identical TGA profile, with a main decomposition step taking place at 340–476 °C, and a maximum decomposition rate of 2%/°C appearing at 409 °C. This peak temperature is in accordance with the decomposition profiles of PET found in the literature (Brems et al., 2011; Ko et al., 2014). Although the r-PET electrospun mat consisted of very fine fibers with much larger surface area than the small pieces of the starting r-PET, it seems that the nanoscale dimension plays no role in its decomposition profile. The reason is that r-PET melts at 250.9 °C, much earlier than the onset of decomposition. Therefore, by the time the material reaches 340 °C, the nanofibers have been transformed into a shapeless melt (see Fig. S1(b) and (c) in the SM). The decomposition continues at higher temperatures until the residual weight reaches almost 0% at 900 °C. In the case of r-PET

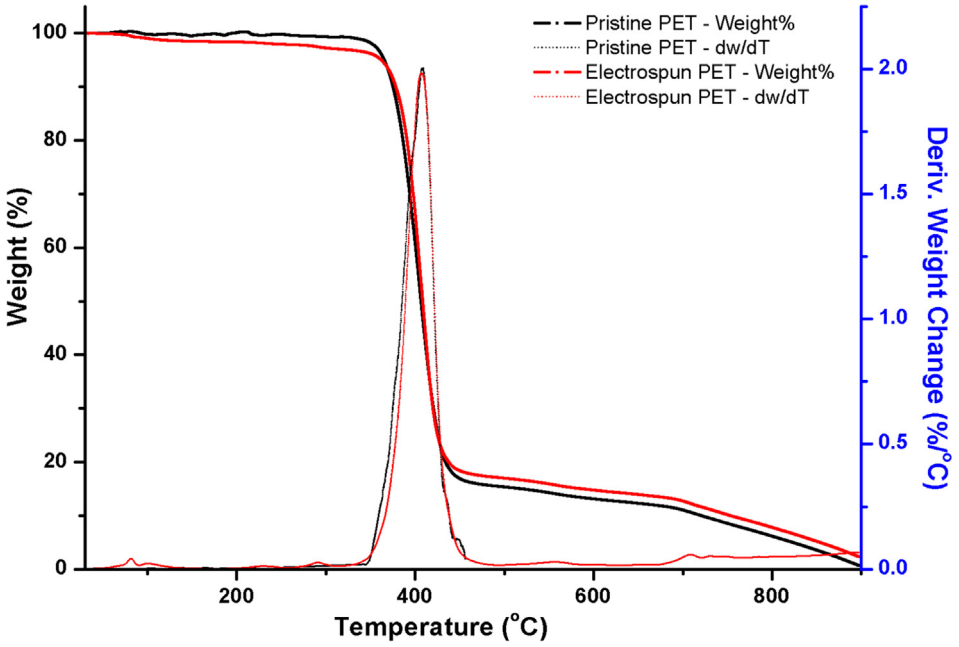

Fig. 3. TGA curves of the starting r-PET and of the electrospun r-PET nanofibers.

it is feasible to produce electrospun mats of varying average fiber diameter using r-PET alone. Nevertheless, due to the melting of these mats at 250.9 °C, they all lose their filamentous structure and they decompose at a similar rate at 409 °C.

3.2. Carbonization of lignin/r-PET nanofibers – the effect of the nanoscale dimension

Understanding the carbonization of electrospun lignin/r-PET fibers is crucial for the preparation of tailor-made carbon nanofibers with a well-formed structure. In order to examine the effect of lowering the diameter to the nanoscale, electrospun samples of varying average fiber diameter were prepared and their TGA curves are presented in Figs. 4 and 5.

In the figures, the TGA profiles of six electrospun samples consisting of fibers with average diameter of 80, 121, 245, 387, 547 and 781 nm respectively are displayed. All samples were prepared using a lignin/r-PET mass ratio of 1/1. Here, it is apparent that the fibers decompose in distinctive steps, which correspond to the regimes found in pristine lignin and in r-PET. The first major step is located between 180 and 260 °C and is attributed to the decomposition of lignin; this is followed by a smaller regime around 300 °C, similar to the one appearing in electrosprayed lignin. In the region between 325 and 460 °C, the major decomposition of

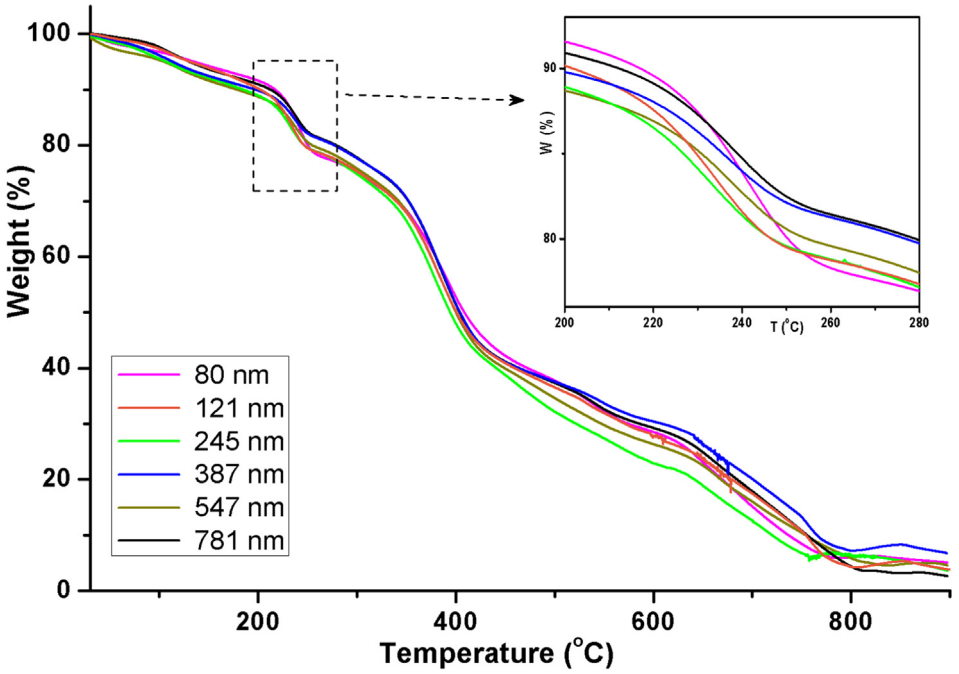

Fig. 4. Weight loss as a function of temperature for electrospun lignin/r-PET fibrous samples of varying average fiber diameter.

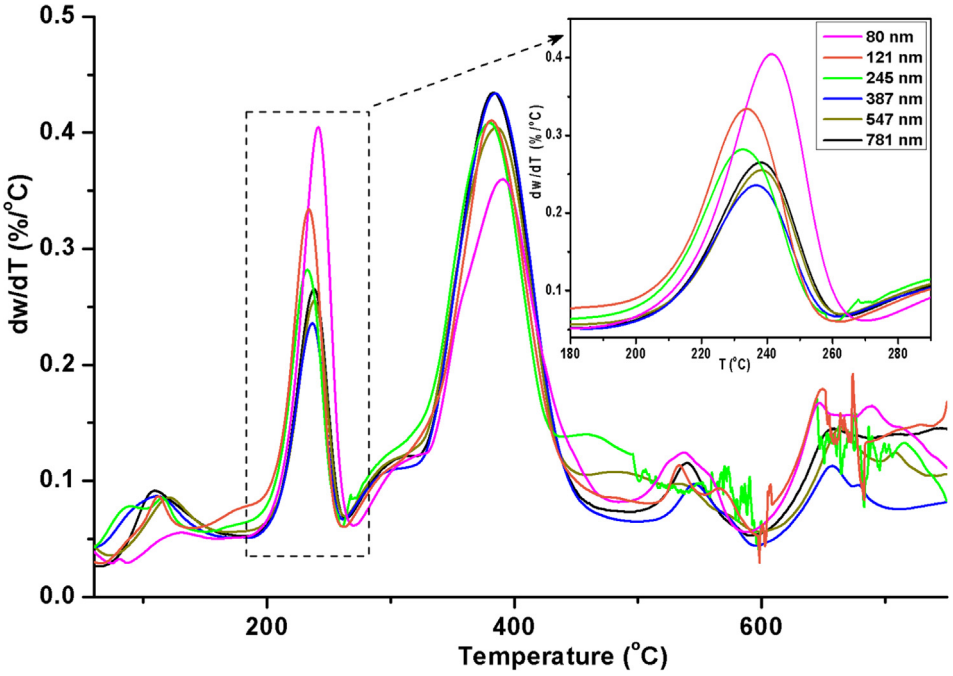

Fig. 5. DTG curves of the electrospun lignin/r-PET fibrous mats.

the r-PET chains take place. Finally, there are two more decomposition regimes, one located between 500 and 600 °C and another one at higher temperatures; both are mainly attributed to lignin.

The effect of lowering the average fiber diameter to the nanoscale is explicit in the first decomposition regime of lignin (180–260 °C). The relatively thicker fibers (387–781 nm) exhibit a peak of maximum decomposition rate of 0.24–0.26%/°C (Fig. 5). However, a higher peak is observed as the diameter decreases. For the fibers of 245 nm the decomposition rate reaches a peak value of 0.28%/°C, and for those of 121 nm their decomposition rate reaches a peak of 0.33%/°C. Furthermore, the thinnest fibers (80 nm) exhibit the highest peak in this region, as their decomposition rate reaches a maximum of 0.40%/°C. This is around 60% higher than the maximum decomposition rate of thicker fibers (>387 nm). These values refer to the peak in the decomposition rate exhibited by the samples in this region, not to the average rate. However, if a comparison based on the average rate is performed, then the thinnest fibers will again have the highest value, as it is reflected in the weight loss measured in this region. For fibers of 387–781 nm, the weight loss between 180 and 260 °C is around 8.5–9.3%. Fibers of 245 nm exhibit a weight loss of 10.3%, those of 121 exhibit a weight loss of 11.3%, and the maximum weight loss in this region is found for the minimum fibers of 80 nm, and it is measured 14.5%. These numbers are concisely presented in Fig. 6.

As already mentioned, the carbonization of the electrospun fibers is a process involving restrictions due to heat and mass transfer. From the previous observations, we can conclude that these restrictions are dominant in fibers of relatively larger diameter (>387 nm). The transfer of heat towards the interior of the fiber and the evolution of volatiles from its core due to diffusion obviously limit the rate of decomposition, to a value that is almost constant over a wide range of diameters (387–781 nm). However, as the average diameter is reduced to less than 245 nm, it seems that these restrictions diminish. Reaching the minimum diameter of 80 nm, these limitations play a minimum role, and here it seems that the overall rate of the process is mainly controlled by the decomposition reactions taking place inside and on the surface of the nanofibers, as the volatile products can be transported more

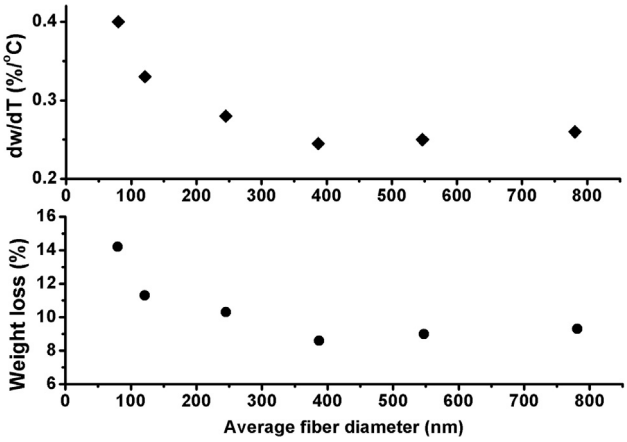

Fig. 6. The influence of the average fiber diameter in the maximum decomposition rate (%/°C) and in the weight loss (%) of the precursor fibers in the region 180–260 °C.

easily to the atmosphere. This effect for the decomposition of nanofibers, although rational, has scarcely been reported. Ye et al. (2015) have presented a higher weight loss for PAN-based electrospun nanofibers of 39 nm average diameter compared to thicker nanofibers, although their study was focused on different aspects.

During carbonization, a higher specific surface area is expected to facilitate the heat transfer towards the interior of the fibers and the mass transfer of the decomposition products to the atmosphere through molecular diffusion. Moreover, a sample of higher surface area will have more molecules exposed on its surface, which can more easily undergo decomposition. Assuming nanofibrous mats of equal mass, prepared from the same raw material, with fibers of a uniform cylindrical shape, and using simple calculations based on their geometry, one can calculate that a relatively small decrease in the average fiber diameter will have a large impact on their total length and specific surface area (see Table S3 and

Fig. S3 in the SM for indicative calculations). Specifically, the electrospun nanofibers with average diameter of 80 nm are 128% longer than those of 121 nm, 838% longer than those of 245 nm and 2240% longer that those of 387 nm. Moreover, the sample having average diameter of 80 nm will theoretically have 51% higher external surface area than the sample of 121 nm, 206% higher external surface area than the one of 245 nm, and 383% higher than the one of 387 nm (assuming that the electrospun nanofibers are not porous, a valid assumption here). Finally, considering the ratio of surface to volume, which shows the number of molecules exposed on the surface compared to those confined in the bulk, the sample of 80 nm will also have 50%, 206% and 383% higher ratio compared to the samples of 121, 245 and 387 nm respectively. Comparisons with the samples which are made of thicker fibers, reveal a much larger difference. The fact that the samples consist of fibers, which have a distribution of diameters over a wider range, doesn't influence so much these calculations, as the samples exhibit a similar fiber distribution with standard deviation around 30–40% of the average diameter.

Regarding the decomposition regime of r-PET, which appears between 325 and 470 °C, having a peak at around 383 °C, it seems in Fig. 5 that the sample of 80 nm shows a lower decomposition rate than the rest. However, its peak is broader to the right, and calculations regarding the % weight loss show that it is similar for all samples in this region, around 31–33%. This amount is lower than the total % of r-PET mass present in each sample (50%). This means that due to the presence of lignin and the intermolecular interactions between these polymers, not all the r-PET decomposes in this region. Instead, a part of it decomposes at higher temperatures.

The differences in the decomposition noticed among the samples with respect to their average fiber diameter, can be observed by examining their SEM images after their carbonization at 600 °C under N_2. Fig. 7(a)–(f) present these results, comparing between the precursor electrospun (on the left) and the same sample after carbonization (on the right). Here, only the samples of 547, 387, and 80 nm are presented, as typical examples of this behavior. The SEM images of the samples 781, 245 and 121 nm, which also indicate this behavior, can be found in the SM (Fig. S2). According to our experience, carbonizing at even higher temperature (e.g. at 800 °C) doesn't change the morphology of the fibrous mat.

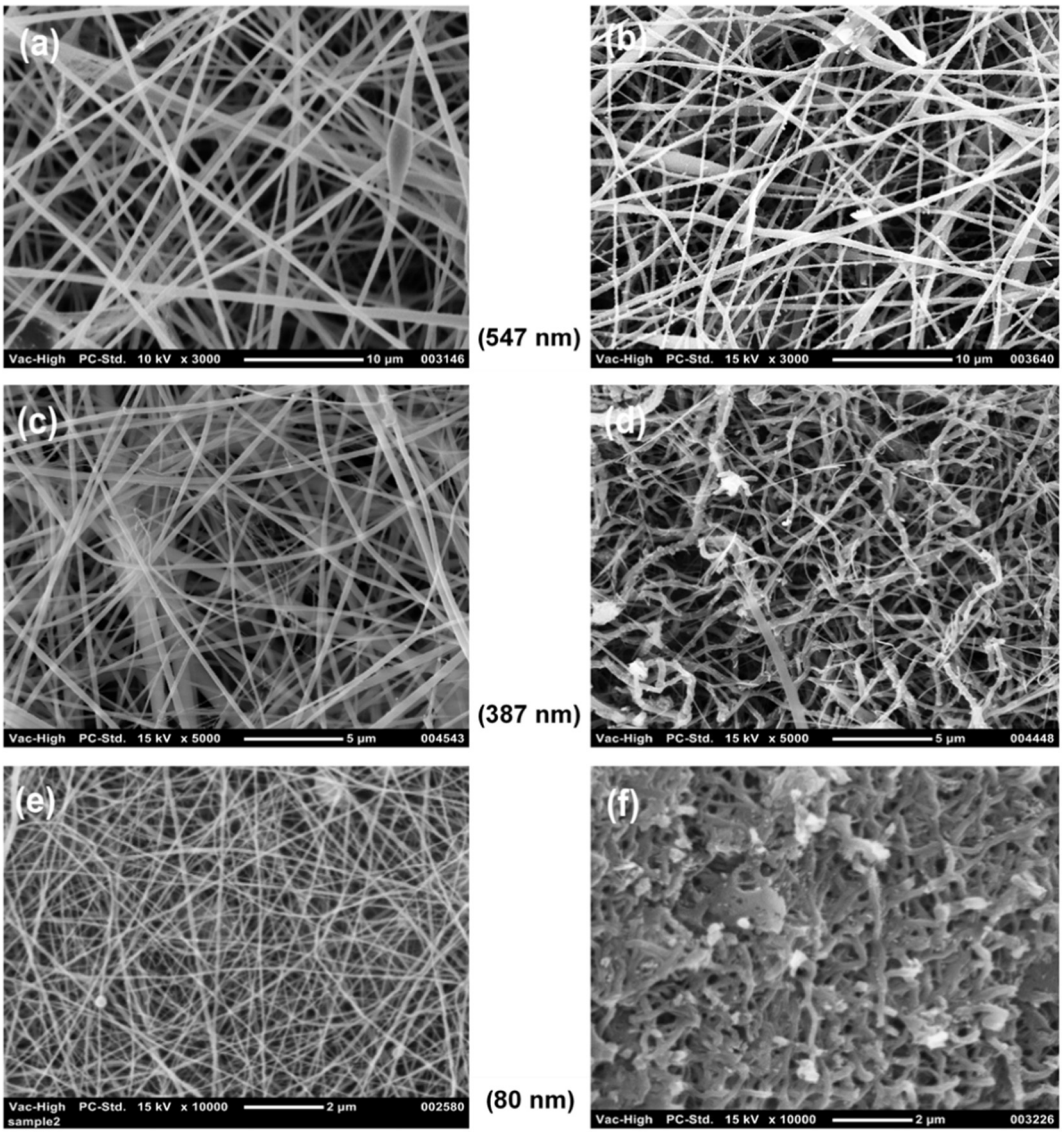

Fig. 7. Carbonization results for the electrospun lignin/r-PET fibrous mats of different average fiber diameter. The precursor mats are presented on the left, and the corresponding carbonized ones on the right; (a)–(b) 547 nm, (c)–(d) 387 nm, (e)–(f) 80 nm, Magnification: images (a)–(b): ×3000, images (c)–(d): ×5000, images (e)–(f): ×10,000.

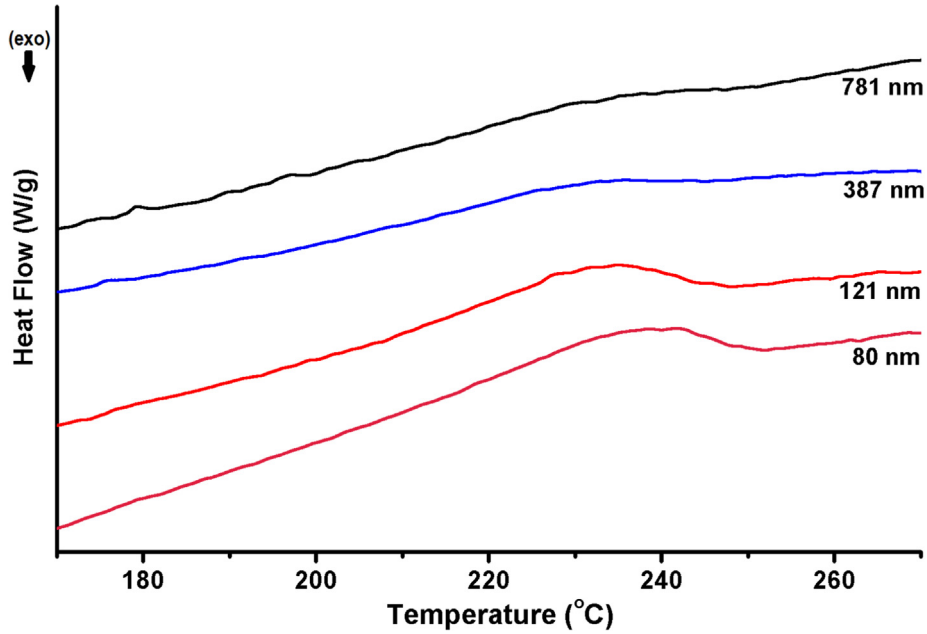

Fig. 8. DSC curves of the samples with average fiber diameter of 80, 121, 387 and 781 nm, after they were heated up to 300 °C.

As the SEM images suggest, the effect of the average fiber diameter, which was observed in the TGA, has an impact on the shape of the carbonized fibers. The samples of relatively larger average diameter (>387 nm) retain their fibrous structure during carbonization. There is no obvious melting or perhaps only at a minor degree, which doesn't destroy the original cylindrical form of the fibers. The final carbon fibers have average diameter at the same levels as the precursors (see Table S2 in the SM for detailed measurements and diameter distributions). However, as the diameter is lowered to the nanoscale, there seems to be melting and fusion of the fibers. The sample of 121 nm shows a considerable degree of melting (see Fig. S2 in the SM), while in the sample of the minimum diameter (80 nm) the melting and fusing is so extensive that the structure cannot be characterized as "fibrous". This melting is expected to have an impact on the surface area of the fibers and to compromise their applicability in relevant applications. It must be mentioned here, that the addition of a "stabilization" step of heating in air before carbonizing them under inert atmosphere, did not prevent the fibers from fusing, although it has been reported effective in other types of lignin-based fibers (Frank et al., 2014; Ruiz-Rosas et al., 2010).

In our previous studies (Svinterikos and Zuburtikudis, 2016), we have shown that lignin and PET are fully miscible. PET itself is a semicrystalline polymer with melting point at 250.9 °C, while lignin is amorphous. When the two polymers are mixed, lignin disrupts the integrity of the PET spherulites as it is intercalated among the PET chains and restricts their movement. However, and based on the results from the TGA studies, it seems that the decomposition of the lignin macromolecules occurring at 180–260 °C gives the chance to PET chains to gain some mobility. This result is more pronounced in the nanofibers of 80 nm, where the decomposition rate is much higher. Therefore, a visible melting behavior appears to some extent, and it results in the fusion among the nanofibers of the minimum average diameter. Heating these nanofibers under N_2 with the same heating rate until just 300 °C reveals that the melting has already occurred at that temperature and that it has destroyed the fibrous network (see Fig. S4 in the SM). This means that the fusion of the nanofibers is manifested at the region of lignin decomposition for the above-mentioned reasons. In contrast, there is no visible melting and fusion in the samples of thicker fibers.

The hypothesis, that the decomposition of lignin up to 300 °C results in an increased mobility of the PET chains and therefore in the melting of the nanofibers, was tested using DSC. Four of the samples were heated one after the other inside the tubular furnace at standard heating rate (5 °C/min) up to 300 °C, without holding them at that temperature, and then they were left to cool down. The whole process was carried out under N_2 atmosphere. The four samples were those with average fiber diameter of 80, 121, 387 and 781 nm respectively. After they cooled down, their DSC curves were recorded and are presented in Fig. 8.

The DSC curves illuminate the differences in the carbonization behavior of the samples based on their diameter. It seems that the samples of small diameter (80 and 121 nm) exhibit clear melting peaks in the region of 230–240 °C. Both peaks are very broad, indicating a non-uniformity of the melting regions. The enthalpy of melting for both samples was measured to be around 1.1–1.2 J/g. In contrast, for the samples of large diameter, the melting peak is much less pronounced, and almost undetectable. For both samples, integration of the curve at this region gave an enthalpy of melting of around 0.4 J/g. This value is much lower than that of the samples of small diameter. Hence, there are much fewer regions inside the material that melt. This observation confirms the hypothesis that the increased decomposition of lignin up to 300 °C in the minimum-diameter nanofibers is responsible for their more pronounced melting, compared to the thicker fibers.

In addition, besides the melting of fibers observed microscopically in the nanofibrous mats of minimum diameter when they are heated, macroscopically these samples show a larger shrinkage and warp compared to those consisting of thicker fibers, and they become more brittle during carbonization (see Fig. S5 in the SM, for the samples heated up to 300 °C). This behavior denotes that during their heating more volatiles are evolved, their hydrogen and oxygen content is reduced more rapidly, and in the end, they yield a stiffer material consisting of a higher percentage of carbon. This assumption was validated and confirmed by performing elemental analysis using EDS for the samples of 80 nm and 781 nm, after they were heated at 320, 490 and 800 °C under inert atmosphere

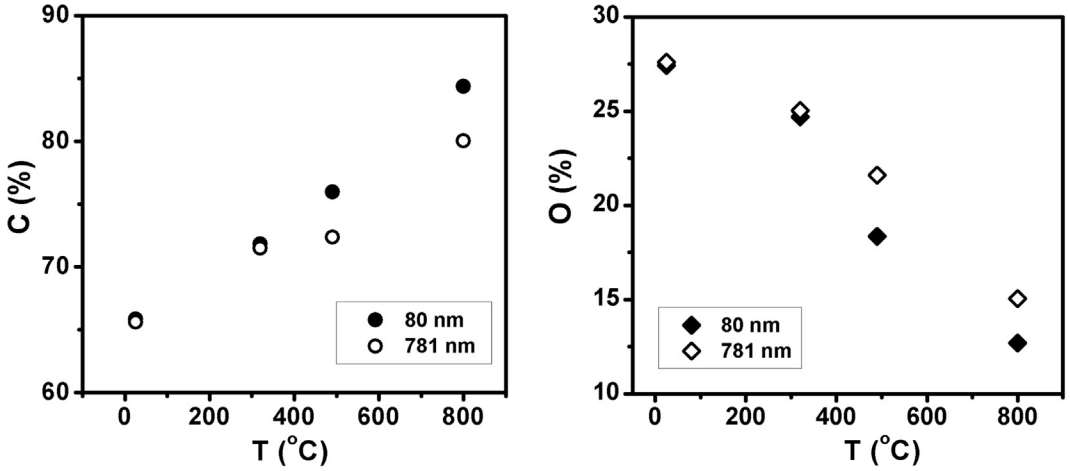

Fig. 9. C % and O % content of the samples of minimum and maximum average diameter, as they are heated under N_2 atmosphere up to 800 °C.

(Fig. 9). This analysis reveals that as these samples are heated, the carbon content in the sample of minimum diameter becomes gradually higher than that of the sample of maximum diameter at the same temperature, while the oxygen content becomes progressively lower. The EDS spectrum of each heated sample can be found in section 8 of the SM.

Currently we are working on the investigation of the nano-dimension effect at different mass ratios of lignin/r-PET, and the results will be presented in a future article.

4. Conclusions

The impact of the nano-dimension on the carbonization process has scarcely been reported in the relevant literature. Here we have demonstrated this effect in the carbonization of electrospun fibers consisting of lignin/r-PET with mass ratio of 1/1. Precursor fibers with average diameter larger than 387 nm show an almost stable decomposition rate (0.24–0.26%/°C) between 180 and 260 °C, the region of lignin decomposition, and yield well-formed carbon fibers. In contrast, minimizing the average diameter of the precursor nanofibrous mats to 80 nm results in the maximum thermal degradation rate (0.40%/°C) and weight loss between 180 and 260 °C, and in the fusion of nanofibers. The reason is that at such low nano-dimensions the heat and mass transfer limitations are not determinant of the process, as many more macromolecules are located on the surface of the fibers. Therefore, lignin decomposes faster, and as a consequence the mobility of PET macromolecules becomes less restricted and the nanofibers merge with each other.

These results underline the importance of taking into account the effect of the nano-dimension, when the manufacture of fine carbon nanofibers is required. Since the carbonization process depends on heat and mass transfer phenomena, the outcome can be considerably influenced by the nano-diameter. The results presented here can, therefore, serve as a road-map for the successful preparation of carbon nanofibers not only from lignin/r-PET, but from other precursor materials, as well, in the framework of sustainability.

Conflict of interest

The authors declare that they have no known competing financial interests or personal relationships that could have appeared to influence the work reported in this paper.

Acknowledgements

The authors would like to acknowledge the financial support provided by the Emirates Center for Energy and Environment Research (ECEER).

Appendix A. Supplementary material

Supplementary data to this article can be found online at https://doi.org/10.1016/j.ces.2019.03.013.

References

Brems, A., Baeyens, J., Beerlandt, J., Dewil, R., 2011. Thermogravimetric pyrolysis of waste polyethylene-terephthalate and polystyrene: a critical assessment of kinetics modelling. Resour. Conserv. Recycl. 55, 772. https://doi.org/10.1016/j.resconrec.2011.03.003.

Chen, T., Zhang, J., Wu, J., 2016. Kinetic and energy production analysis of pyrolysis of lignocellulosic biomass using a three-parallel Gaussian reaction model. Bioresour. Technol. 211, 502. https://doi.org/10.1016/j.biortech.2016.03.091.

Chin, B., Fui, L., Yusup, S., Al Shoaibi, A., 2014. Kinetic studies of co-pyrolysis of rubber seed shell with high density polyethylene using thermogravimetric approach. Energy Convers. Manage. 87, 1. https://doi.org/10.1016/j.enconman.2014.07.043.

Compere, A.L., Griffith, W.L., Leitten, C.F., Pickel, J.M., 2005. Evaluation of lignin from alkaline-pulped hardwood black liquor, Vol. 118; ISBN 1800553684, <http://web.ornl.gov/info/reports/2005/3445605475900.pdf>.

Dallmeyer, I., Ko, F., Kadla, J.F., 2010. Electrospinning of technical lignins for the production of fibrous networks. J. Wood Chem. Technol. 30, 315. https://doi.org/10.1080/02773813.2010.527782.

Frank, E., Steudle, L.M., Ingildeev, D., Spörl, J.M., Buchmeiser, M.R., 2014. Carbon fibers: precursor systems, processing, structure, and properties. Angew. Chem. Int. Ed. 53, 5262. https://doi.org/10.1002/anie.201306129.

García, A., Toledano, A., Serrano, L., Egüés, I., González, M., Marín, F., Labidi, J., 2009. Characterization of lignins obtained by selective precipitation. Sep. Purif. Technol. 68, 193.

Inagaki, M., Yang, Y., Kang, F., 2012. Carbon nanofibers prepared via electrospinning. Adv. Mater. 24, 2547. https://doi.org/10.1002/adma.201104940.

Kim, J., Kim, K.-H., Kwon, E.E., 2016. Enhanced thermal cracking of VOCs evolved from the thermal degradation of lignin using CO2. Energy 100, 51. https://doi.org/10.1016/j.energy.2016.01.075.

Ko, K., Rawal, A., Sahajwalla, V., 2014. Analysis of thermal degradation kinetics and carbon structure changes of co-pyrolysis between macadamia nut shell and PET using thermogravimetric analysis and 13 C solid state nuclear magnetic resonance. Energy Convers. Manage. 86, 154. https://doi.org/10.1016/j.enconman.2014.04.060.

Ko, F., Wan, Y., 2014. Introduction to Nanofiber Materials. Cambridge University Press, New York. chapter 3.

Kubo, S., Kadla, J.F., 2005. Lignin-based carbon fibers: effect of synthetic polymer blending on fiber properties. J. Polym. Environ. 13, 97. https://doi.org/10.1007/s10924-005-2941-0.

Mohabeer, C., Abdelouahed, L., Marcotte, S., Taouk, B., 2017. Comparative analysis of pyrolytic liquid products of beech wood, flax shives and woody biomass

components. J. Anal. Appl. Pyrolysis 127, 269. https://doi.org/10.1016/j.jaap.2017.07.025.
NAPCOR – National association for PET container resources of USA, (n.d.). <http://www.napcor.com/PET/landing_petrecycling.html>. (accessed 20 October 2018).
Ogale, A., Zhang Meng, J., Jin, J., 2016. Recent advances in carbon fibers derived from biobased precursors. J. Appl. Polym. Sci. 133. https://doi.org/10.1002/app.44212.
Peng, S., Li, L., Kong, J., Lee, Y., Tian, L., Srinivasan, M., Adams, S., 2016. Electrospun carbon nanofibers and their hybrid composites as advanced materials for energy conversion and storage. Nano Energy 22, 361. https://doi.org/10.1016/j.nanoen.2016.02.001.
Przepiórski, J., Karolczyk, J., Takeda, K., Tsumura, T., Toyoda, M., Morawski, A.W., 2009. Porous carbon obtained by carbonization of PET mixed with basic magnesium carbonate: pore structure and pore creation mechanism. Ind. Eng. Chem. Res. 48, 7110. https://doi.org/10.1021/ie801694t.
Rodríguez Correa, C., Stollovsky, M., Hehr, T., Rauscher, Y., Rolli, B., Kruse, A., 2017. Influence of the carbonization process on activated carbon properties from lignin and lignin-rich biomasses. ACS Sustain. Chem. Eng. 5, 8222. https://doi.org/10.1021/acssuschemeng.7b01895.
Ruiz-Rosas, R., Bedia, J., Lallave, M., Loscertales, I.G., Barrero, A., Rodríguez-Mirasol, J., Cordero, T., 2010. The production of submicron diameter carbon fibers by the electrospinning of lignin. Carbon N. Y. 48, 696. https://doi.org/10.1016/j.carbon.2009.10.014.
Svinterikos, E., Zuburtikudis, I., 2016. Carbon nanofibers from renewable bioresources (lignin) and a recycled commodity polymer [poly(ethylene terephthalate)]. J. Appl. Polym. Sci. 133, 43936. https://doi.org/10.1002/app.43936.
Svinterikos, E., Zuburtikudis, I., 2017. Tailor-made electrospun nanofibers of biowaste lignin/recycled poly(ethylene terephthalate). J. Polym. Environ. 25, 465. https://doi.org/10.1007/s10924-016-0806-3.
Ye, J.S., Liu, Z.T., Lai, C.C., Lo, C.T., Lee, C.L., 2015. Diameter effect of electrospun carbon fiber support for the catalysis of Pt nanoparticles in glucose oxidation. Chem. Eng. J. 283, 304. https://doi.org/10.1016/j.cej.2015.07.071.
Zhang, B., Kang, F., Tarascon, J., Kim, J., 2016. Recent advances in electrospun carbon nanofibers and their application in electrochemical energy storage. Prog. Mater. Sci. 76, 319. https://doi.org/10.1016/j.pmatsci.2015.08.002.